DE-Vol. 84-1, 1995 Design Engineering Technical Conferences
Volume 3 — Part A
ASME 1995

DYNAMICS OF A NONLINEAR PARAMETRICALLY-EXCITED PARTIAL DIFFERENTIAL EQUATION

Richard H. Rand
Dept. of Theoretical & Applied Mechanics
Cornell University
Ithaca, New York

William I. Newman
Depts. of Earth & Space Sciences,
Physics & Astronomy, & Mathematics
University of California
Los Angeles, California

Bruce C. Denardo
Department of Physics and Astronomy
University of Mississippi
University, Mississippi

Alice L. Newman
Department of Physics
California State University, Dominguez Hills
Carson, California

ABSTRACT

We investigate a nonlinear Mathieu equation with diffusion and damping, using both perturbation theory and numerical integration. The perturbation results predict that for parameters which lie near the 2 : 1 resonance tongue of instability corresponding to a mode shape $\cos nx$, the resonant mode achieves a stable periodic motion, while all the other modes are predicted to decay to zero. By numerically integrating the p.d.e. as well as a 3-mode o.d.e. truncation, the predictions of perturbation theory are shown to represent an oversimplified picture of the dynamics. In particular it is shown that steady states exist which involve many modes. The dependence of steady state behavior on parameter values and initial conditions is investigated numerically.

INTRODUCTION

This work concerns the dynamical behavior of the following partial differential equation:

$$\frac{\partial^2 u}{\partial t^2} - c^2 \frac{\partial^2 u}{\partial x^2} + \epsilon\beta \frac{\partial u}{\partial t} + [\delta + \epsilon\gamma \cos t]\, u = \epsilon\alpha u^3 \quad (1)$$

with the boundary conditions

$$\frac{\partial u}{\partial x} = 0 \quad \text{at} \quad x = 0 \quad \text{and} \quad x = \pi \quad (2)$$

Our study is motivated by two experiments which were part of author Denardo's Ph.D. thesis at UCLA (Denardo, 1990; Denardo et al., 1990; Denardo et al., 1992): (i) a line of coupled pendula with vertical forcing, and (ii) water waves in a vertically forced channel. Eqs. (1) and (2) represent an approximate model of these systems, and our ultimate aim is to compare the predictions of the model with the experimental results. The purpose of the present paper, however, is to compare a perturbation treatment of these equations (valid for small ϵ), with a direct numerical integration of the p.d.e.

Eq. (1) may be thought of as a generalization of the Mathieu equation,

$$\frac{d^2 u}{dt^2} + [\delta + \epsilon \cos t]\, u = 0 \quad (3)$$

to which nonlinear ($\epsilon\alpha u^3$), damping ($\epsilon\beta \partial u/\partial t$), and diffusive ($c^2 \partial^2 u/\partial x^2$) terms have been added. Eq. (3) has been studied by many authors. For example, Stoker (1950) presents a perturbation approach valid for small ϵ to discuss the dynamics of eq. (3) in the neighborhood of 2 : 1 resonance, $\delta = 1/4 + O(\epsilon)$, i.e., when the forcing frequency (= 1) is nearly twice the natural frequency ($= \sqrt{\delta} \approx 1/2$). The well-known result is that the rest solution $u \equiv 0$ is unstable for

$$\left|\delta - \frac{1}{4}\right| \leq \frac{\epsilon}{2} + O(\epsilon^2) \quad (4)$$

and stable for all other parameters near the 2 : 1 resonance. See Fig. 1.

A version of eq. (1) in which diffusive and damping terms have been omitted has been previously studied

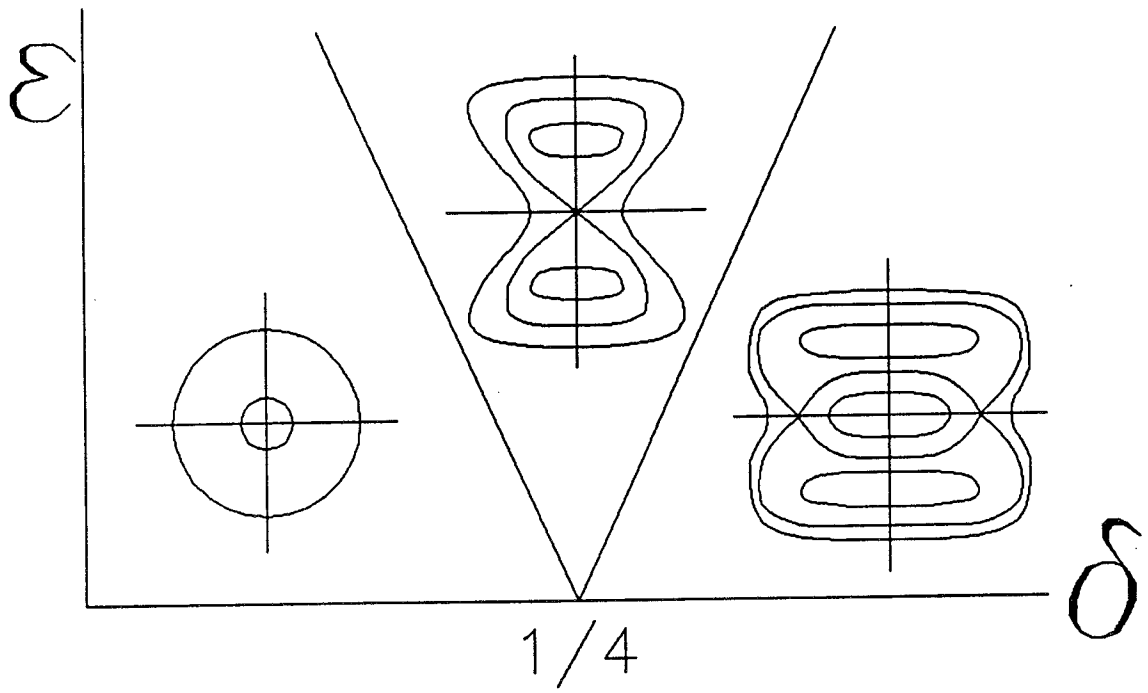

Fig.1. Tongue of instability (4) for eqs.(3),(5) for parameters near the 2:1 resonance at $\delta = 1/4$, $\epsilon = 0$. Displayed are schematic representations of typical Poincare maps in the u–$\dot{u}$ plane for eq.(5) as obtained by perturbation theory (Holmes and Rand, 1981; Month and Rand, 1982).

by Nayfeh and Mook (1979), Holmes and Rand (1981), and Month and Rand (1982), namely

$$\frac{d^2u}{dt^2} + [\delta + \epsilon \cos t]\, u = \epsilon\alpha u^3 \qquad (5)$$

These authors used perturbation methods valid for small ϵ and restricted to a neighborhood of $2:1$ resonance, $\delta = 1/4 + O(\epsilon)$, to discuss the effect of the nonlinear term $\epsilon\alpha u^3$ on Mathieu's eq. (3). It was found that for $\alpha > 0$, $0 < \epsilon << 1$, there are 0, 1, or 2 periodic solutions in addition to the trivial solution $u \equiv 0$, depending on the values of δ and ϵ:

$\delta - \frac{1}{4} \leq -\frac{\epsilon}{2}$ 0 periodic solutions

$-\frac{\epsilon}{2} < \delta - \frac{1}{4} < \frac{\epsilon}{2}$ 1 periodic solution (stable)

$\frac{\epsilon}{2} \leq \delta - \frac{1}{4}$ 2 periodic solutions (1 stable, 1 unstable)

See Fig. 1, where the Poincaré map associated with a surface of section $\sum : t = 0 \bmod 2\pi$ is displayed for each of these three cases. The effect of the nonlinear term $\epsilon\alpha u^3$ may be described in words as follows: The region of instability (4) associated with the linear Mathieu eq. (3) persists, but the unbounded growth which occurs in (3) is replaced by a finite amplitude periodic motion. The nonlinearity gives rise to an amplitude-dependent shift in frequency of the unforced system which may be thought of as balancing the parametric resonance. The effect of including a damping term $\epsilon\beta\, du/dt$ is to break the saddle connections in Fig. 1, and to change the centers into sinks.

The foregoing discussion summarizes the perturbation results for the o.d.e. version of eq. (1), i.e., eq. (1) when $c = 0$ or when $u(x,t)$ is a function of time alone. In the rest of this paper we shall be interested in the effects of including a diffusive term $c^2\, \partial^2 u/\partial x^2$. In the next section we develop a perturbation solution to eq. (1) comparable to the perturbation approaches obtained previously for the o.d.e. version of eq. (1). Then we compare the predictions of the perturbation method with direct numerical integration of the p.d.e. (1) and of systems of o.d.e. truncations of (1).

PERTURBATION METHOD

In order to satisfy the boundary conditions (2), we assume a solution in the form of an infinite series

$$u = f_0(t) + f_1(t)\cos x + f_2(t)\cos 2x + \ldots \qquad (6)$$

Substituting (6) into (1) and simplifying the trigonometric terms in u^3 gives

$$\ddot{f}_n + \omega_n^2 f_n + \epsilon\left(\beta\dot{f}_n + \gamma f_n \cos t\right) = \epsilon\alpha g_n \qquad (7)$$

where $\omega_n^2 = \delta + n^2c^2$ and where g_n is a cubic in all the f_i's. For example, the expression for g_0 obtained by using MACSYMA after truncating terms beyond f_6 is

$$g_0 = \frac{3}{2}f_0f_6^2 + \frac{3}{2}f_1f_5f_6 + \frac{3}{2}f_2f_4f_6 + \frac{3}{4}f_3^2f_6 + \frac{3}{2}f_0f_5^2$$
$$+\frac{3}{2}f_1f_4f_5 + \frac{3}{2}f_2f_3f_5 + \frac{3}{2}f_0f_4^2 + \frac{3}{2}f_1f_3f_4 + \frac{3}{4}f_2^2f_4$$
$$+\frac{3}{2}f_0f_3^2 + \frac{3}{2}f_1f_2f_3 + \frac{3}{2}f_0f_2^2 + \frac{3}{4}f_1^2f_2 + \frac{3}{2}f_0f_1^2 + f_0^3 + \ldots$$

For convenience in what follows, we write (7) in the abbreviated form

$$\ddot{f}_n + \omega_n^2 f_n = \epsilon Q_n \qquad (8)$$

where $Q_n = -\beta\dot{f}_n - \gamma f_n \cos t + \alpha g_n$.

When $\epsilon = 0$, the solution to (8) may be written

$$f_n = R_n \cos(\omega_n t + \psi_n) \qquad (9)$$

where R_n and ψ_n are constants. When $\epsilon > 0$, we look for a solution to (8) in the form (9) with R_n and ψ_n as functions of t (variation of parameters).

As is well-known (Rand 1994), R_n and ψ_n satisfy the differential equations

$$\dot{R}_n = -\epsilon\frac{Q_n}{\omega_n}\sin(\omega_n t + \psi_n) \qquad (10)$$

$$R_n\dot{\psi}_n = -\epsilon\frac{Q_n}{\omega_n}\cos(\omega_n t + \psi_n) \qquad (11)$$

Next we use the method of averaging to replace eqs. (10) and (11) by simpler, though approximate equations, a procedure which is valid for small ϵ. We omit the details of the computation, which involves replacing the right hand sides of (10) and (11) with their average values (averaged in t, holding R_n and ψ_n fixed).

For general (nonresonant) values of the parameters, eq. (10) on R_n averages to

$$\dot{R}_n = -\epsilon\frac{\beta}{2}R_n \qquad (12)$$

All solutions to (12) decay to zero. We thus come to the first conclusion, namely that *unless we are in the neighborhood of a resonance* (to be discussed next), *all motions are predicted to damp out.*

If, however, $\omega_n = 1/2$, then there will be an extra term in the averaged eq. (12), namely

$$\dot{R}_n = -\epsilon\frac{\beta}{2}R_n + \epsilon\frac{\gamma}{2}R_n \sin 2\psi_n \qquad (13)$$

Since $\omega_n^2 = \delta + n^2c^2$, such a resonance relation can exist for only a single value of n (for fixed values of δ and c).

Thus in the case of such a resonance, *all modes except the resonant mode* will have averaged equations of the form (12), i.e., they *will decay to zero.*

In order to find out what happens to the resonant mode, we have to examine the averaged version of eq. (11) on ψ_n. Before doing so, we generalize the discussion to allow for detuning from resonance, that is

$$\omega_n^2 = \frac{1}{4} + \Delta\epsilon \tag{14}$$

where Δ is a detuning coefficient.

In computing the averaged version of eq. (11) on the resonant mode ψ_n, we use the fact that the amplitudes R_i of all the nonresonant modes decay to zero, and we restrict attention to the long-time behavior. In doing so we obtain simplified equations for ψ_n, which are valid after the transients associated with the decay of the nonresonant modes die out, namely

$$\dot{\psi}_n = \epsilon\Delta + \epsilon\frac{\gamma}{2}\cos 2\psi_n - \frac{9}{16}\epsilon\alpha R_n^2, \quad n > 0 \tag{15}$$

$$\dot{\psi}_0 = \epsilon\Delta + \epsilon\frac{\gamma}{2}\cos 2\psi_0 - \frac{3}{4}\epsilon\alpha R_0^2, \quad n = 0 \tag{16}$$

STEADY STATE RESONANCE

The averaged equations governing resonance are eqs. (13), (15), and (16). At steady state these slow flows will approach their stable equilibria, each equilibrium corresponding to a periodic motion of the original system. These will satisfy the eqs.:

$$\beta = \gamma \sin 2\psi_n \tag{17}$$

$$\Delta + \frac{\gamma}{2}\cos 2\psi_n - \frac{9}{16}\alpha R_n^2 = 0, \; n > 0 \tag{18}$$

$$\Delta + \frac{\gamma}{2}\cos 2\psi_0 - \frac{3}{4}\alpha R_0^2 = 0, \; n = 0 \tag{19}$$

From (17) we see that $\sin 2\psi_n = \beta/\gamma$. Substituting this into (18) and (19), we obtain the steady state amplitudes

$$R_n^2 = \frac{16}{9\alpha}\left[\Delta \pm \frac{1}{2}\sqrt{\gamma^2 - \beta^2}\right], \quad n > 0 \tag{20}$$

$$R_0^2 = \frac{4}{3\alpha}\left[\Delta \pm \frac{1}{2}\sqrt{\gamma^2 - \beta^2}\right], \quad n = 0 \tag{21}$$

As an example, take the case where the damping β is zero, and where $n > 0$. Then

$$R_n^2 = \frac{16}{9\alpha}\left[\Delta \pm \frac{1}{2}\gamma\right], \quad n > 0 \tag{22}$$

But R_n^2 must be nonnegative. This gives that there will be 0, 1, or 2 solutions (in addition to the trivial solution $R_n = 0$), depending on Δ, hence

$$\Delta < -\gamma/2 \rightarrow \text{ 0 periodic solutions} \tag{23}$$

$$-\gamma/2 < \Delta < \gamma/2 \rightarrow \text{ 1 periodic solution} \tag{24}$$

$$\Delta > \gamma/2 \rightarrow \text{ 2 periodic solutions} \tag{25}$$

It turns out that these changes in the number of periodic solutions coincide with changes in stability of the trivial solution $R_n = 0$ (as may be shown by considering the slow flow linearized near $R_n = 0$.) In cases (23) and (25), the trivial solution is stable, while it is unstable in the case of (24). In (24), the nontrivial periodic solution is stable, while in (25) one of the nontrivial periodic solutions is stable, and one is unstable. In cases (24) and (25), the stable motion corresponds to the + sign in eqs. (20) and (21).

If there is small damping, the results are similar, except the stable equilibria of the slow flow change from centers to sinks. These stable periodic solutions are the unique asymptotic state for given values of the parameters, independent of initial conditions, except if two stable states coexist [as in (25), where the rest solution $u \equiv 0$ is also stable].

Now suppose that we fix the values of the parameters α, β, γ, and ϵ, and ask how the steady state dynamics of eqs. (1), (2) change as δ and c are varied. We refer the reader to Fig. 2 which shows the resonances

$$\omega_n^2 = \delta + n^2c^2 = \frac{1}{4} \tag{26}$$

for $n = 0, 1, 2, 3, 4$ plotted in the $\delta - c$ plane. The perturbation analysis is valid in the neighborhood of each of these curves, and predicts that a stable periodic motion of the form

$$u(x,t) = R_n \cos(\omega_n t + \psi_n)\cos nx \tag{27}$$

where R_n and ψ_n are constants [cf. eqs. (20) and (21)], exists on these curves.

In the case of detuning, cf. eq. (14), each resonance curve has a region in its neighborhood in which the rest solution $u \equiv 0$ is unstable. See Fig. 3. The boundaries of these instability regions (or Arnold tongues) are given by $\Delta = \pm\sqrt{\gamma^2 - \beta^2}/2$, cf. (20),(21), or by

$$\delta + n^2c^2 = \frac{1}{4} \pm \frac{\sqrt{\gamma^2 - \beta^2}}{2}\epsilon + O(\epsilon^2) \tag{28}$$

For points inside these regions, a stable periodic motion of the form (27) is predicted to exist. For $\alpha > 0$, points

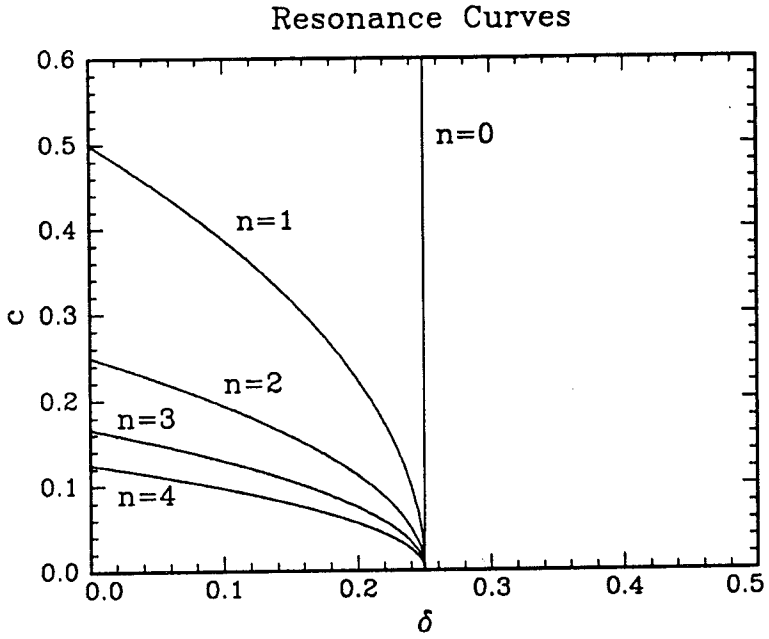

Fig.2. The resonance curves of eq.(26) for n = 0,1,2,3,4.

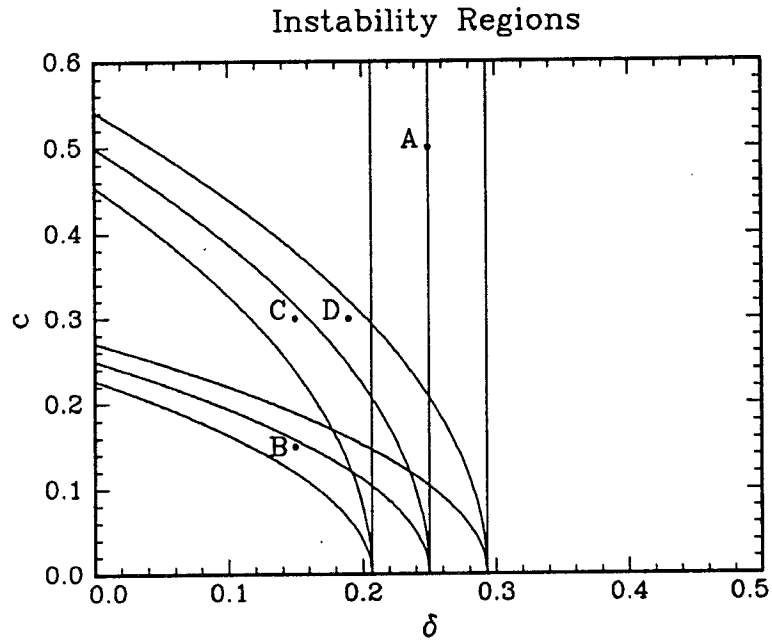

Fig.3. The instability regions of eq.(28) and the resonance curves of eq.(26) for $\beta = 1/2$, $\gamma = 1$, $\epsilon = 0.1$ and n = 0,1,2. The points A,B,C,D refer to example systems discussed in the text.

lying outside a region (28), but on its right-hand side, are predicted to involve two stable states (a periodic solution of known amplitude, and the trivial solution). For points outside of (28) on its left-hand side, however, only the trivial solution is stable. In the case where two stable solutions exist, the question of which one occurs depends on the initial conditions.

Note that while the resonance curves (26) intersect only at $\delta = 1/4$, $c = 0$, the associated instability regions (28) overlap. At points in the overlap regions, we may expect that periodic motions of the form (27) exist for each of the values of n corresponding to each of the overlapping regions.

Thus the perturbation theory gives a charmingly simple picture of the steady state dynamics of eqs. (1) and (2), at least for small ϵ and in the neighborhood of $2:1$ resonance. The rest of this paper consists of a comparison between these predictions and the actual behavior of the p.d.e. (1) as obtained by numerical integration.

NUMERICAL INTEGRATION OF THE P.D.E.

In order to simulate the p.d.e. (1) we used the "method of lines" (Jones et al., 1972). The basic feature of this method is that the derivatives with respect to one of the independent variables (i.e. time) remain continuous, while derivatives with respect to the other independent variables are replaced by finite-difference approximations. The method of lines is essentially a technique for replacing a system of partial differential equations by a system of ordinary differential equations, like pseudospectral methods, using local Taylor series (in contrast with Fourier series) to develop the expansion. Employing a computational grid for the method of lines with the same resolution as that employed in an earlier 128 point pseudospectral expansion produced results which were identical over four significant figures over 100 oscillation periods of the system.

We generally chose our initial conditions in the form

$$u(x,0) = a_0 + a_1 \cos x + a_2 \cos 2x \qquad u_t(x,0) = 0 \tag{29}$$

where we specified the initial Fourier components a_0, a_1 and a_2. We numerically integrated the system (1) and (2) for 800 time units or greater, at which point steady state was approximately achieved. Then we Fourier expanded in x the numerical solution to obtain

$$u(x,t) = f_0(t) + f_1(t)\cos x + f_2(t)\cos 2x + \ldots + f_{20}(t)\cos 20x \tag{30}$$

where $f_n(t)$ is the Fourier component with wave number n.

In order to restrict the complexity of the problem, all of the numerical experiments which we report here correspond to the parameter values

$$\alpha = 1, \quad \beta = \frac{1}{2}, \quad \gamma = 1, \quad \epsilon = 0.1 \tag{31}$$

For these fixed parameter values, we vary δ and c as well as the initial conditions (29).

A comparison of the predictions of the perturbation approach with the results of numerical integration may be illustrated with some examples. We present results for four typical points labeled A, B, C, D in Fig. 3. In each case initial conditions (29) are taken in the form

$$u(x,0) = 0.1 + 0.1\cos x + 0.1\cos 2x \qquad u_t(x,0) = 0 \tag{32}$$

For point A: $(\delta, c) = (0.25, 0.5)$, numerical integration produced a periodic motion with all $f_n(t) \equiv 0$ except $f_0(t)$, which had amplitude 0.77. To compare this result with perturbation theory, we note that since $\delta = 0.25$, the detuning Δ of $\omega_0^2 = \delta = 0.25$ in eq. (14) is zero, so that the predicted amplitude R_0 of the $n = 0$ mode in eq. (21) is given by $R_0 = 0.76$.

For point B: $(\delta, c) = (0.15, 0.15)$, numerical integration produced a periodic motion with all $f_n(t) \equiv 0$ except $f_2(t)$, which had amplitude 0.78. This time the detuning of $\omega_2^2 = \delta + 4c^2 = 0.24$ is given by $\Delta = -0.1$, yielding predicted amplitude $R_2 = 0.77$ in eq. (20).

For point C: $(\delta, c) = (0.15, 0.3)$, numerical integration produced a periodic motion with all even modes $f_{2n}(t) \equiv 0$, while $f_1(t)$ had amplitude 0.78, $f_3(t)$ had amplitude 0.01 and the other odd modes had amplitude ≤ 0.001. This time the detuning of $\omega_1^2 = \delta + c^2 = 0.24$ is given by $\Delta = -0.1$, yielding predicted amplitude $R_1 = 0.77$ in eq. (20).

Thus there is excellent agreement between perturbation theory and numerical integration for points A, B, and C. Not so for point D, however.

For point D: $(\delta, c) = (0.19, 0.3)$, numerical integration produced a quasiperiodic motion with all modes present. See Fig. 4. The approximate amplitudes of $f_0(t)$, $f_1(t)$, $f_2(t)$ are respectively given by 0.3, 0.9, 0.3, although these values vary slightly from cycle to cycle since the motion is not periodic. The corresponding amplitudes of the higher modes are all ≤ 0.03. We shall refer to this steady state as a *multimode* response. The frequencies of the modes $n = 0, 1, 2$ (which also vary from cycle to cycle) are approximately found to

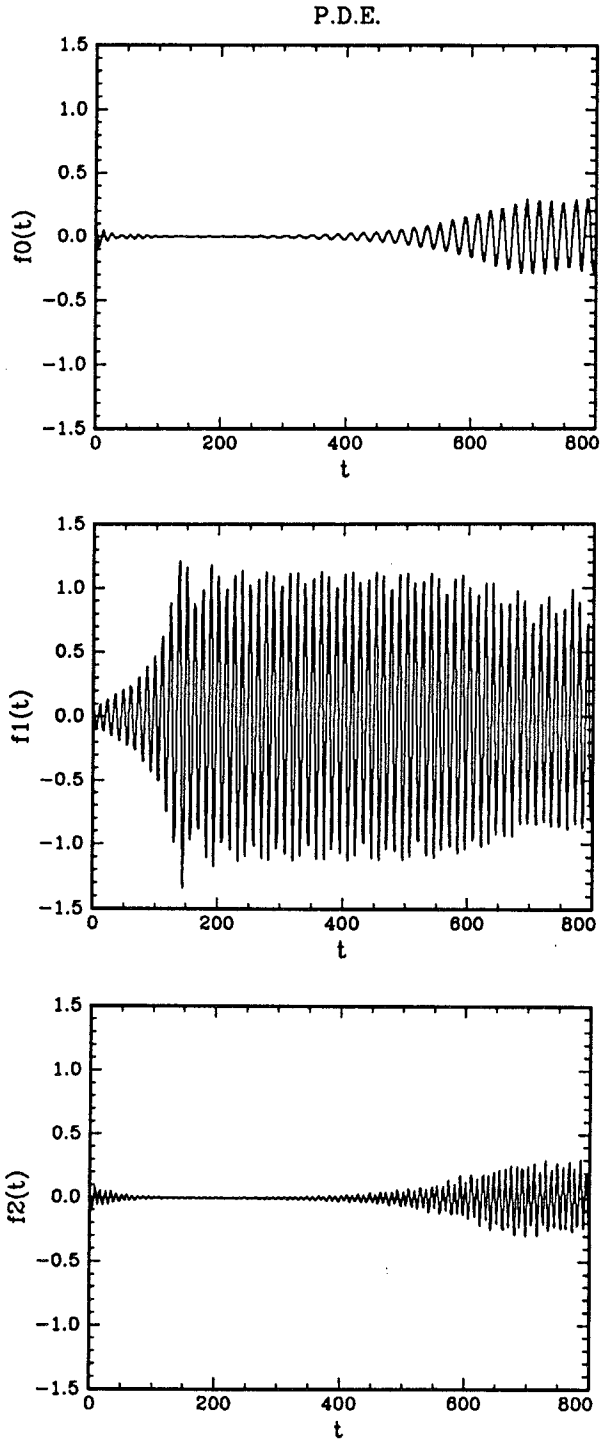

Fig.4. Numerical integration of the p.d.e. (1),(2). The functions $f_n(t)$ are the Fourier components of eq.(30). Parameters correspond to point D in Fig.3, cf.eqs.(31),(32). Note the multimode behavior of the steady state.

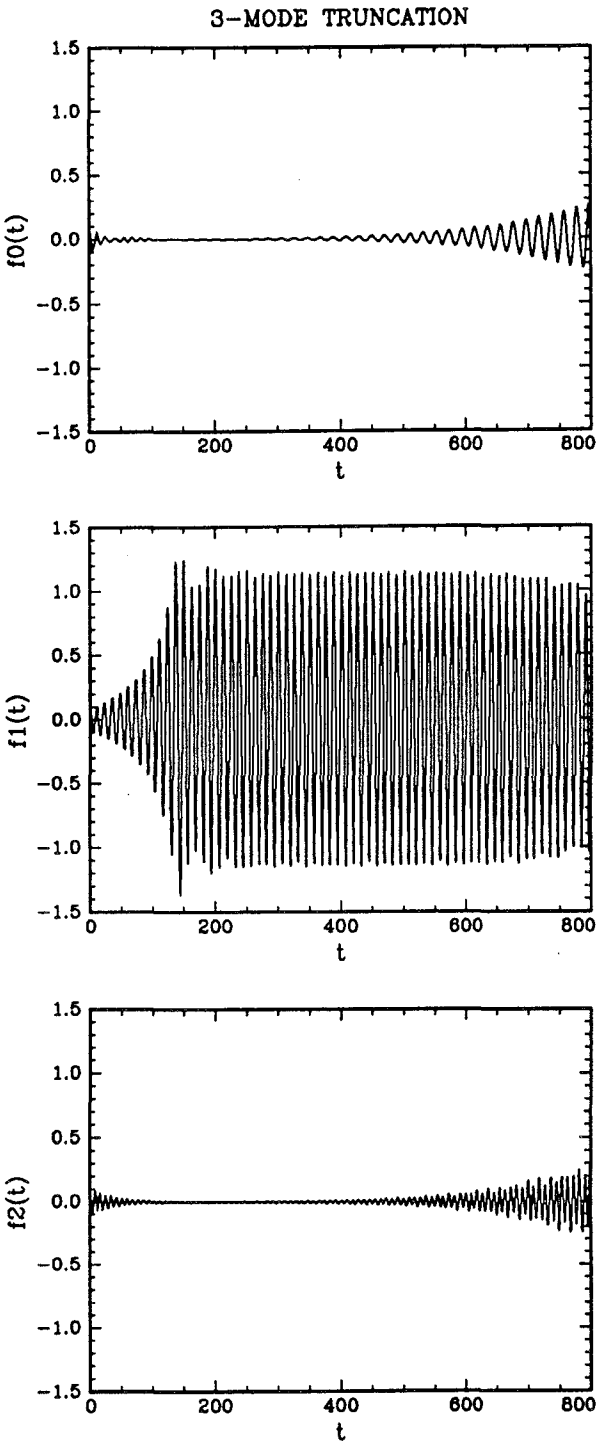

Fig.5. Numerical integration of the three–mode o.d.e. truncation (34)–(36). Parameters and initial conditions are the same as for Fig.4.

be $\omega_0 = 0.33$, $\omega_1 = 0.5$, $\omega_2 = 0.67$, and hence represent a resonance in the ratio

$$\omega_0 : \omega_1 : \omega_2 : \omega_d :: 2 : 3 : 4 : 6 \qquad (33)$$

where $\omega_d = 1$ is the frequency of the driver $\cos t$. In this case the perturbation result is completely wrong: the detuning of $\omega_1^2 = \delta + c^2 = 0.28$ is given by $\Delta = 0.3$, yielding the predicted amplitude of a lone periodic $n = 1$ mode of $R_1 = 1.14$ in eq. (20). No such lone $n = 1$ mode is observed.

Another feature which is present in the dynamics of the p.d.e., but which is missing from the perturbation theory, is the possibility of unbounded growth. The presence of the nonlinearity in the form $\epsilon\alpha u^3$ is responsible for this phenomenon, in contrast to a more realistic nonlinearity of the form $\sin u$. The absence of unbounded growth from the perturbation theory may be due to the scaling by small ϵ, which localizes the dynamics around the origin $u \equiv 0$.

THREE-MODE TRUNCATION

Another feature observed in our numerical experiments is that, generally speaking, the steady state is dependent on the initial conditions. This phenomenon is well known in finite dimensional problems, i.e., in systems of o.d.e.'s. A familiar example is a 2π-periodically forced single degree of freedom oscillator, where the dependency of steady state on initial conditions may be displayed by giving the boundaries of the basins of attraction on a Poincaré section with cut at $t = 0 \bmod 2\pi$ (see Hsu (1987) for example). The present situation is much more complicated, however, because of the infinite dimensional nature of the dynamics, i.e., we may think of the p.d.e. (1) as a system of an infinite number of coupled oscillators, each corresponding to a single mode $\cos nx$.

In order to investigate the dependency of steady state on initial conditions in an efficient manner, we consider a three mode o.d.e. truncation of the infinite system (7)

$$\ddot{f}_0 + \omega_0^2 f_0 + \epsilon(\beta \dot{f}_0 + \gamma f_0 \cos t) = \epsilon\alpha \left[f_0^3 + \frac{3}{2} f_0 f_2^2 + \frac{3}{4} f_1^2 f_2 + \frac{3}{2} f_0 f_1^2 \right] \qquad (34)$$

$$\ddot{f}_1 + \omega_1^2 f_1 + \epsilon(\beta \dot{f}_1 + \gamma f_1 \cos t) = \epsilon\alpha \left[3 f_0^2 f_1 + \frac{3}{4} f_1^3 + \frac{3}{2} f_1 f_2^2 + 3 f_0 f_1 f_2 \right] \qquad (35)$$

$$\ddot{f}_2 + \omega_2^2 f_2 + \epsilon(\beta \dot{f}_2 + \gamma f_2 \cos t) = \epsilon\alpha \left[3 f_0^2 f_2 + \frac{3}{4} f_2^3 + \frac{3}{2} f_1^2 f_2 + \frac{3}{2} f_0 f_1^2 \right] \qquad (36)$$

where $\omega_0^2 = \delta$, $\omega_1^2 = \delta + c^2$ and $\omega_2^2 = \delta + 4c^2$.

Here we have selected 3 modes (rather than 2 or 4, say) because the multimode response (33) observed in the p.d.e. chiefly involved 3 modes.

Numerical simulation of the truncated system (34)–(36) by a fourth-order Runge-Kutta has shown that it gives a good approximation of the p.d.e. (1) and (2) for some parameters and for initial conditions of the form (29). For example see Fig. 5, which shows that the 3-mode truncation exhibits the multimode behavior of Fig. 4.

We numerically integrated eqs. (34)–(36) for a wide range of parameter values, and for each of four sets of initial conditions: $(f_0(0), f_1(0), f_2(0)) = (0.1, 0.1, 0.1), (1.0, 0.1, 0.1), (0.1, 1.0, 0.1), (0.1, 0.1, 1.0)$, the results of which are respectively displayed in Figs. 6-9. All four of these Figures use the following symbols to denote the observed steady state:

0:	f_0 only,	$f_1 = f_2 = 0$
1:	f_1 only,	$f_0 = f_2 = 0$
2:	f_2 only,	$f_0 = f_1 = 0$
–:	trivial solution,	$f_0 = f_1 = f_2 = 0$
X:	unbounded growth	
A:	f_0 and f_1 only,	$f_2 = 0$
B:	f_1 and f_2 only,	$f_0 = 0$
C:	f_0 and f_2 only,	$f_1 = 0$
M:	f_0, f_1 and f_2 all present	(multimode)

Table 1: Symbols used in Figs.6-9.

In all cases the initial velocities were taken as zero for simplicity. We note that in addition to the trivial motion and to the pure modes predicted by perturbation theory, a variety of mixed modes are observed, as well as unbounded growth. Comparison of Figs.6-9 shows that the dynamics of the truncated system (34)–(36) is very complicated, far more complicated than the simple picture coming from the perturbation theory presented above. Although the dynamics of the truncated system is surely not exactly the same as the dynamics of the p.d.e. (1) and (2), it gives us an indication of the great complexity of the steady state structure of the p.d.e.

DISCUSSION AND CONCLUSIONS

Inspection of Fig. 6, which corresponds to initial conditions which lie relatively close to the origin, clearly

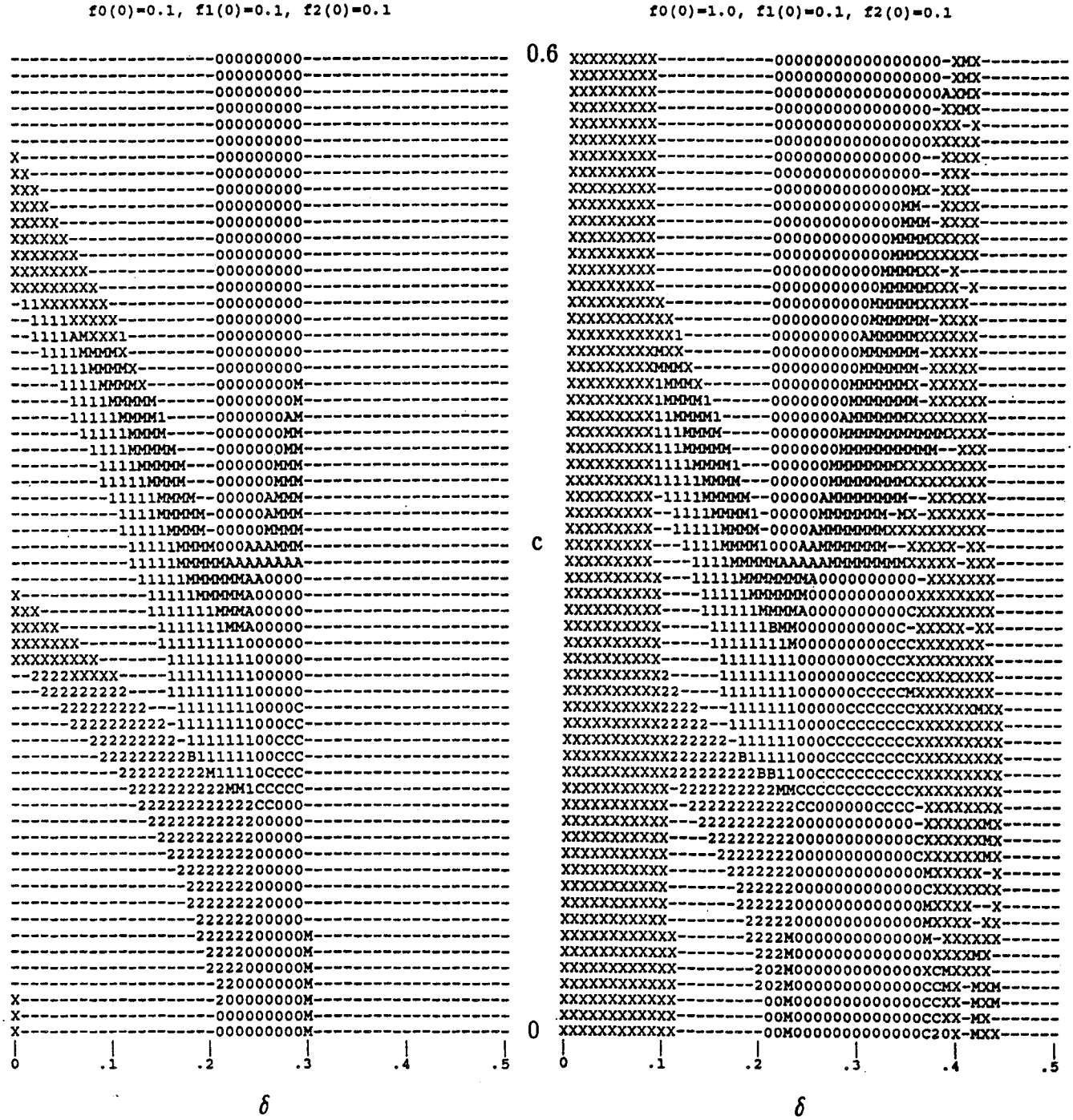

Figs.6 and 7. Results of numerical integration of the three–mode o.d.e. truncation for parameters (31). The resulting steady states are represented by a variety of symbols given in Table 1.

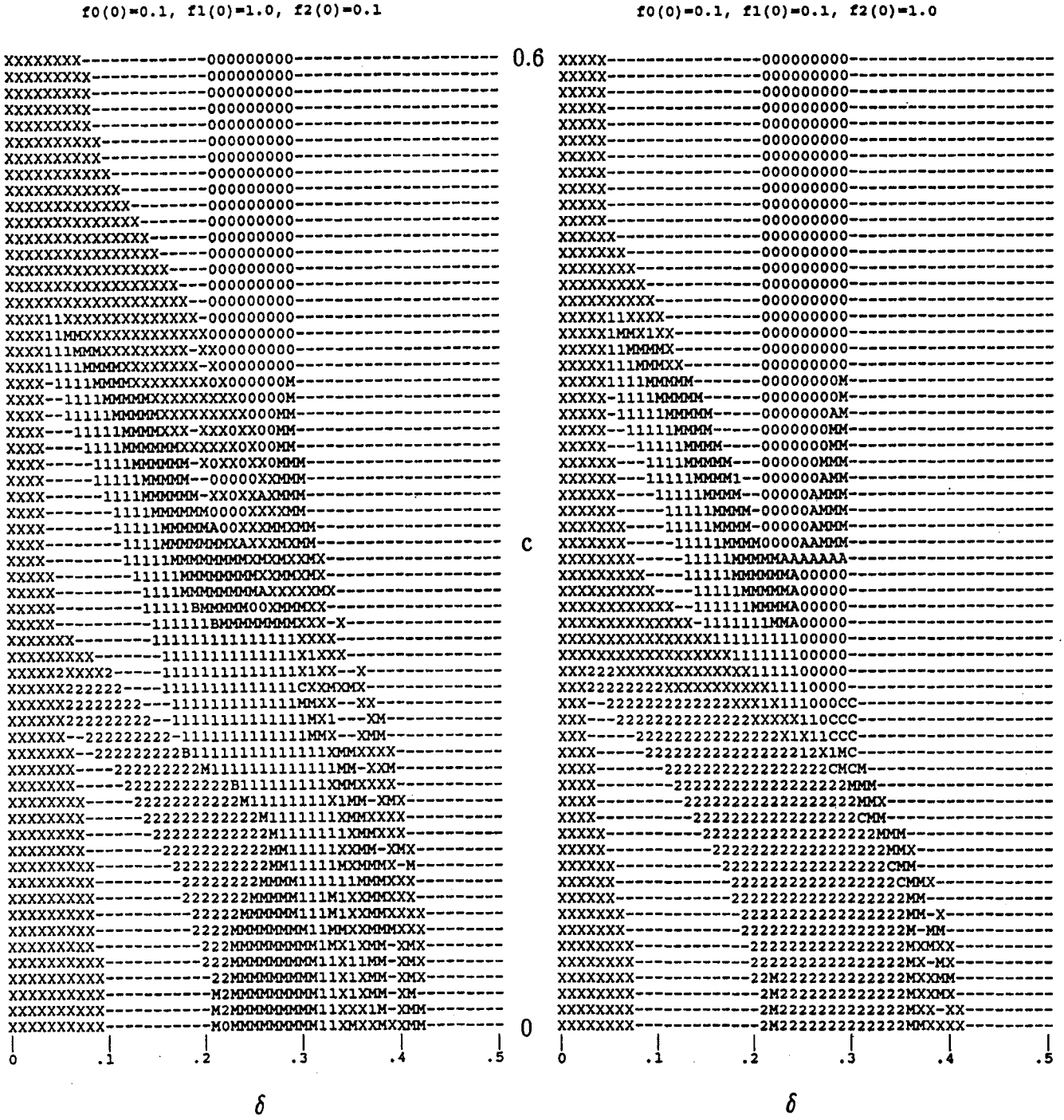

Figs.8 and 9. Results of numerical integration of the three–mode o.d.e. truncation for parameters (31). The resulting steady states are represented by a variety of symbols given in Table 1.

shows the regions of instability predicted by perturbation theory, cf. Fig. 3. Parameter values which lie outside these instability regions are seen to correspond to the trivial steady state (displayed as the symbol "–"), in agreement with perturbation theory. Parameter values which lie inside the instability regions are predicted by perturbation theory to lead to a lone periodic resonant mode (displayed by one of the symbols "0," "1" or "2"). Although this prediction is fulfilled in Fig. 6 for some points inside the instability regions, there are also observed a number of multimode steady states (displayed by one of the symbols "*A*," "*B*," "*C*" or "*M*"). In addition, some motions are observed to lead to unbounded growth (displayed by the symbol "*X*").

In contrast with Fig. 6, Figs. 7, 8, and 9 correspond to a relatively large initial condition in one of the modal amplitudes (respectively f_0, f_1, f_2), while the other two initial conditions remain small. Figs. 7–9 have less in common with the predictions of perturbation theory than that exhibited by Fig. 6. At parameters lying outside of the regions of instability predicted by perturbation theory, the larger initial conditions of Figs. 7–9 have led to steady states other than the trivial solution. In addition, unbounded growth is seen to occur for a wider range of parameter values. Note that in each of Figs. 7-9, the mode which is given the larger initial condition (respectively 0, 1, and 2) occurs more plentifully than in Fig. 6, especially to the right of the associated region of instability predicted by perturbation theory. This is to be expected since such an initial condition is likely to lie in the interior of the basin of attraction of the respective steady state. Note also that the steady states which involve only two components (symbolized by "*A*," "*B*" and "*C*") often lie near the boundaries of the tongues associated with their respective components.

In this paper we have compared the predictions of a perturbation analysis of a parametrically excited *p.d.e.* with numerical integration of the *p.d.e.* and of a three-term *o.d.e.* truncation. The relationship between the all too simple picture presented by the perturbation method and the extremely complicated behavior of the p.d.e. is itself complicated. The tongues of instability predicted by the perturbation theory are present in the numerically observed dynamics, but we have observed multimode steady states which are absent from the present perturbation results.

The three-term o.d.e. truncation shares some of the complexity of the p.d.e. We may view the truncated approximation as an autonomous system of four coupled o.d.e.'s (by associating the $\cos t$ forcing term with the output of a simple harmonic oscillator). Although we know of no general study of four coupled oscillators, Baesens, Guckenheimer, Kim and MacKay (1991) have shown that the dynamics of three coupled oscillators is extremely complicated.

We view the present paper as a first step in understanding the behavior of the p.d.e. (1) and (2). We expect additional work to be done on this system both because it has numerous applications, as well as because it is a natural extension of Mathieu's equation (3) and thus represents a paradigm system for parametrically excited p.d.e.'s. In particular we hope for a perturbation analysis which yields the nature and bifurcation of the multimode steady states which we have observed numerically.

REFERENCES

Baesens, C., Guckenheimer, J., Kim, S. and MacKay, R.S., 1991, "Three Coupled Oscillators: Mode Locking, Global Bifurcations and Toroidal Chaos," *Physica D*, vol.49, pp.387–475.

Denardo, B., 1990, *Observations of Nonpropagating Oscillatory Solitons*, Ph.D. thesis, Department of Physics, University of California, Los Angeles.

Denardo, B., Galvin, B., Greenfield, A., Larraza, A., Putterman, S. and Wright, W., 1992, "Observations of Localized Structures in Nonlinear Lattices: Domain Walls and Kinks," *Phys. Rev. Let.*, vol.68, pp.1730–1733.

Denardo, B., Wright, W. and Putterman, S., 1990, "Observation of a Kink Soliton on the Surface of a Liquid," *Phys. Rev. Let.*, vol.64, pp.1518–1521.

Holmes, C.A. and Rand, R.H., 1981, "Coupled Oscillators as a Model for Nonlinear Parametric Excitation," *Mechanics Res. Comm.*, vol.8, pp.263–268.

Hsu, C.S., 1987, *Cell-to-Cell Mapping*, Springer, New York.

Jones, D.J., South, J.C. and Klunker, E.B., 1972, "On the Numerical Solution of Elliptic Partial Differential Equations by the Method of Lines," *J. Comp. Phys.*, vol.9, pp.496–527.

Month, L.A. and Rand, R.H., 1982, "Bifurcation of 4:1 Subharmonics in the Nonlinear Mathieu Equation," *Mechanics Res. Comm.*, vol.9, pp.233–240.

Nayfeh, A.H. and Mook, D.T., 1979, *Nonlinear Oscillations*, Wiley, New York.

Rand, R., 1994, *Topics in Nonlinear Dynamics with Computer Algebra*, Gordon and Breach Sicence Publishers, Langhorne, PA.

Stoker, J.J., 1950, *Nonlinear Vibrations in Mechanical and Electrical Systems*, Wiley, New York.